Perturbing GaN/AlN quantum dots with uniaxial stressors

Ofer Moshe[1], Daniel H. Rich[*,1], Benjamin Damilano[2], and Jean Massies[2]

[1] Department of Physics, The Ilse Katz Center for Nano and Meso Scale Science and Technology,
   Ben-Gurion University of the Negev, P.O.B. 653, Beer-Sheva 84105, Israel
[2] Centre de Recherche sur l'Hétéro-Epitaxie et ses Applications, Centre National de la Recherche Scientifique, Rue B. Gregory,
   Sophia Antipolis, 06560 Valbonne, France

* Corresponding author: e-mail danrich@bgu.ac.il, Phone: +972 8 6461648, Fax: +972 8 6472904

We have studied the effect of uniaxial stress on the optical polarization properties of GaN/AlN quantum dots (QDs) grown on Si(111) substrates. Microcracks form as a result of the thermal expansion coefficient mismatch between the GaN/AlN layers and the Si(111) substrate. We show that such microcracks serve as excellent stressors through which the strain tensor of the GaN/AlN QDs can be modified for studies of strain-induced changes in the optical properties using a spatially and temporally resolved probe, such as with cathodoluminescence (CL) imaging and spectroscopy. CL measurements of the ground-state excitonic transition of vertically stacked GaN/AlN quantum dots (QDs) exhibit an in-plane linear polarization anisotropy in close proximity to microcracks, consistent with the presence of uniaxial stress. The spatial dependence of the polarization anisotropy and CL decay time in varying proximity to the microcracks are studied as a function of temperature in order to assess the influence of thermal stress variations on the oscillator strength between electrons and holes.

1 Introduction The high luminescence efficiency in the visible to ultra-violet spectral range of group III-Nitride self-assembled quantum dots (QDs) shows great promise for the fabrication of lasers and light emitting diodes in a wide wavelength range [1–3]. An important issue that remains a topic of interest in this system is the electric field in the QD which originates from piezoelectric and py-roelectric charge polarization. The field is estimated to be ~5 to 7 MV/cm and is mainly oriented along the [0001] direction [4, 5]. A second issue is the choice of suitable substrates on which to grow group III-Nitrides heterostructures [6]. Si is a common substrate that exhibits a large mismatch in thermal expansion coefficient with group III-Nitrides films, and heteroepitaxy can lead to the formation of microcracks in the film during the post-growth cooling of the wafer [7]. While the deleterious nature of microcracks in III-V/Si systems is well known, the microcracks can be exploited to provide limited regions of uniaxial stress for the purpose of measurably perturbing the optical and electronic properties of heterolayer films grown on Si [8].

We recently demonstrated this approach by using microcracks to create μm-scale regions of uniaxial stress that alter the excess carrier lifetimes and optical polarization properties of excitons in GaN/AlN QDs, as probed with spatially and temporally resolved cathodoluminescence (CL) [9, 10]. Thus, microcracks along the high-symmetry ⟨11-20⟩ directions in the III-Nitride on Si(111) system can serve as excellent stressors for the purpose of perturbing the electronic structure in quantum heterolayers and self-assembled QDs by producing μm-scale regions of in-plane uniaxial stress. Previously, uniaxial stresses on the order of ~10-30 kbar have been observed [9, 10]. In this paper, we further build on this approach and present CL results for the temperature dependence of the polarization anisotropy and excitonic lifetime in varying proximity to microcracks for GaN/AlN QDs grown on Si.

Phys. Status Solidi C **6**, No. 6 (2009)

1433

2 Experiment The samples were grown by molecular beam epitaxy using the 2D to 3D Stranski-Krastanov growth mode transition [2, 11, 12]. Two samples were grown on Si(111) substrates and consist of AlN (30 nm)/GaN (400 nm)/AlN (700 nm) buffer layers followed by either 40 or 85 layers of GaN QDs, labeled as samples S40 and S85, respectively. The growth of sample S40 (S85) involved 18-nm (6.7-nm) thick AlN barrier layers with 2.6-nm (1.6-nm) thick GaN dot layers, resulting in an average dot height of ~5 nm (~3.7 nm), as determined previously by transmission electron microscopy measurements for samples possessing very similar structures and growth conditions. Both samples were terminated with a 40-nm thick AlN capping layer. The average dot density is ~3×10^{11} cm^{-2}.

The linearly polarized cathodoluminescence detection system is installed on a JEOL 5910 scanning electron microscope (SEM) with modified ports for an optical system to collect luminescence from samples mounted on a variable temperature stage. An ellipsoidal mirror with variable three-axis positioning collects luminescence emitted from the sample. The emitted luminescence is focused onto a coherent optical fiber bundle with a vacuum rotatable linear polarizer positioned before the fiber optics [8]. Two polarization directions for the polarizer will be denoted with the subscripts $\perp$ and $\parallel$ to indicate detection orientations with E perpendicular and parallel to a microcrack that is oriented along the [11-20] crystallographic direction. The polarization anisotropy ratio, R_p, is defined by the ratio of CL intensities, I, under the two orthogonal polarizer orientations and is given by $R_p = I_\perp/I_\parallel$. The light from the flexible fiber bundle was transferred to a 1/4-meter monochromator outside the SEM vacuum system. The spectral resolution of the monochromator was 2 nm (~15 meV) at $\lambda = 400$ nm (3.10 eV). The dispersed light was detected with a multialkali photomultiplier tube which enabled photon counting. Time-resolved CL experiments were performed with the method of delayed coincidence in an inverted single photon counting mode [13]. Electron beam pulses of 50 ns width with a 100 kHz repetition rate were used to excite the sample.

3 Results and discussion A monochromatic CL image ($\lambda = 476$ nm) and scanning electron microscopy (SEM) image are shown in Fig. 1 for the S40 sample at T = 300 K. Similar images for sample S85 were obtained and therefore not shown here. The electron beam current and energy were, respectively, $I_b = 200$ pA and $E_b = 15$ keV. The effective spatial resolution in CL for these imaging conditions is ~0.3 μm. Long microcracks are evident with orientations in the ⟨11-20⟩ directions, as shown in both CL and SEM images. We note the presence of some smaller microcracks in the SEM image whose features are barely visible in the corresponding CL images. The smaller cracks may represent an incomplete severing of the film and thus will have a reduced effect on the optical properties. We will focus on the effects of the larger microcracks, one of which is shown with a dashed white line intersecting a microcrack along an orthogonal direction, [-1100], in Fig. 1(a).
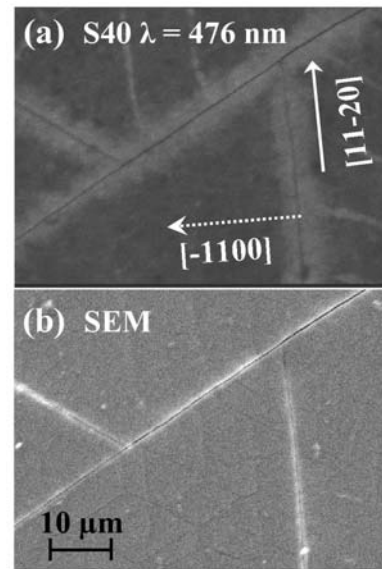

Figure 1 Monochromatic CL image with $\lambda = 476$ nm ($h\nu = 2.605$ eV) in (a) and an SEM image in (b) over the same regions of the S40 sample showing microcracks along the <11-20> directions. The sample temperature was 300 K.

We have performed local CL spectroscopy and lifetime measurements by positioning the e-beam at various points along the [-1100] direction (dashed white line in Fig. 1). Stack plots of local CL spectra for both samples are shown in Fig. 2 for various temperatures, as indicated. For each panel, two vertical stacks are shown for spectra acquired at positions of $\Delta x = 0.5$ μm and $\Delta x = 5$ μm from the microcrack (along the [-1100] direction), representing regions of
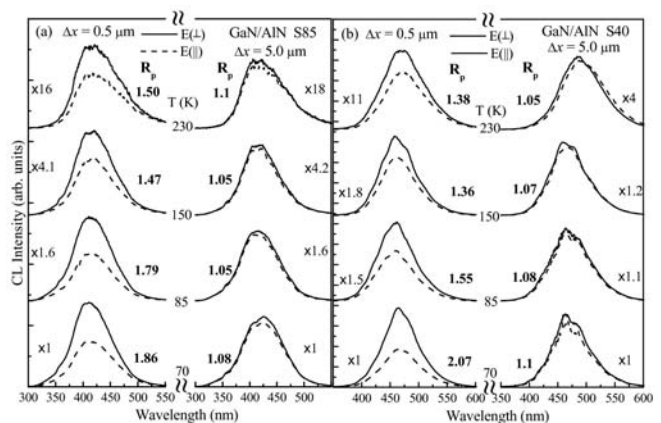
Figure 2 CL spectra acquired locally with the e-beam focused to a spot at various temperatures for samples S-85 and S-40 in (a) and (b), respectively. The CL spectra were acquired at two locations, $\Delta x = 0.5$ μm and $\Delta x = 5.0$ μm, relative to the microcrack. The intensities of some of the spectra have been scaled to more easily facilitate a comparison, as shown. The polarization anisotropy ratio, $R_p = I_\perp/I_\parallel$, for each pair of spectra is indicated.
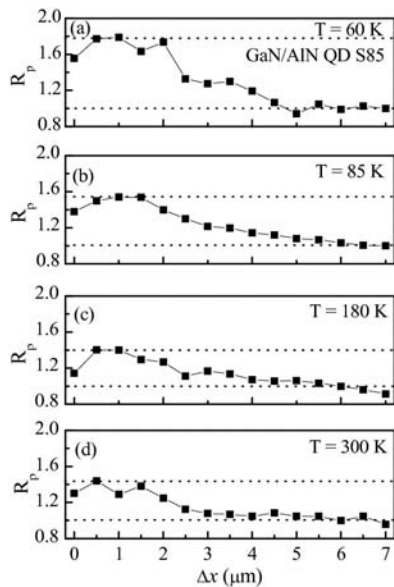
Figure 3 CL line scans of the anisotropy ratio R_p vs distance Δx from a microcrack for samples S85 for the various temperatures shown.

nearly pure uniaxial stress and biaxial stress, respectively. For regions of uniaxial stress ($\Delta x = 0.5$ μm), Fig. 2 shows that R_p increases from ~1.4 (1.5) to ~2.1 (1.9) as the temperature decreases from 230 K to 70 K for sample S40 (S85). For the region where biaxial stress is predominant ($\Delta x = 5$ μm) R_p does not deviate too far from 1. The maximum deviation of ~10% may reflect the presence of defects, dislocations, and smaller cracks which could act to cause some deviation from pure biaxial stress even far from the large microcracks.

We have examined in detail the dependence of R_p as a function of distance (Δx) from a microcrack, as shown in Fig. 3 for sample S85. It is clear that R_p decreases monotonically towards $R_p = 1$ for the various temperatures shown. Again, the maximum value of R_p occurs for the lowest temprature, and this value decreases as the temperature increases. Moreover, the spatial range, W_R, over which R_p deviates from unity changes with temperature. W_R was determined by a linear fit and extrapolation of the decreasing side of the polarization ratio data in Fig. 3 to the expected asymptotic limit of $R_p = 1$. The values of W_R, obtained from linear fits, are shown in Fig. 4 for both samples; typical error bars are indicated. The general trend for both samples is that W_R decreases as the temperature is raised towards 300 K. Some deviations in this trend are observed and may be due to the experimental uncertainties.

The broadening of the range (W_R) from the microcrack at which $R_p > 1$ apparently indicates an enhancement in the range of uniaxial stress at low temperatures due to a further contraction of the GaN/AlN film relative to Si. For distances (Δx) greater than ~6 μm (~4 μm) from the microcrack at both high and low temperatures R_p approaches
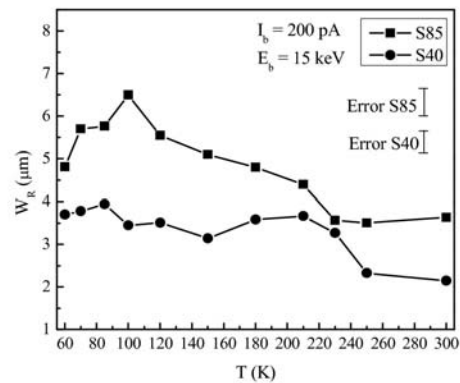
Figure 4 The spatial range, W_R, over which $R_p > 1$ for various temperatures. W_R is a measure of the spatial broadening of the polarization anisotropy relative to a microcrack.

unity for S85 (S40), indicating the presence of biaxial stress in both samples. The measured range over which we observe a transition from uniaxial stress to biaxial stress is also consistent with a similar range ($\Delta x \approx 3$ μm) over which the measured radiative lifetime changes in the S40 and S85 samples, as discussed below. In previous measurements and modeling of these samples, we obtained biaxial tensile stress values of ~30 kbar and ~15 kbar at room temperature for samples S-85 and S-40, respectively. Consequently, the larger values of W_R for S85, in comparison to that for S-40 (as observed for all temperatures in Fig. 4) are further consistent with the larger stress value in S-85.

In a similar way, we have examined the spatial variation in the CL decay time, as shown in Fig. 5. Figures 5(a) and 5(c) show that the CL decay times reduce for both samples by ~50% as the *e*-beam is positioned from the uniaxially stress region near the microcracks to the biaxially stressed regions greater than ~3 μm from the microcracks. Similar results for both high and low temperature measurements indicate that this behavior is roughly independent of temperature. Previously, we attributed this spatial variation of lifetime to a ~50% smaller oscillator strength between electrons and holes for QDs subject to a uniaxial tensile stress relative to the oscillator strength for QDs subject to a biaxial stress, which is accompanied by a 10-15% increase in the electric field for the uniaxially stressed QDs [9, 10]. A more surprising aspect of the lifetime measurements is revealed in Figs. 5(b) and 5(d) which shows the temperature dependence of the decay times. The decay times for S40 in Fig. 5(d) show an increase of ~50% as the temperature is lowered in the range from 300 to 150 K. Such a behavior is expected based on the reduced contribution of the nonradiative components to the overall lifetime. The decay times are however roughly constant for sample S85 in Fig. 5(b) over the same range and may reflect a reduced nonradiative contribution to the lifetime for this sample. Over the range $120 \geq T \geq 60$ K, the decay times for both samples are observed to decrease by a maximum of ~20%. The decrease in the decay time over this low

Phys. Status Solidi C **6**, No. 6 (2009)

1435
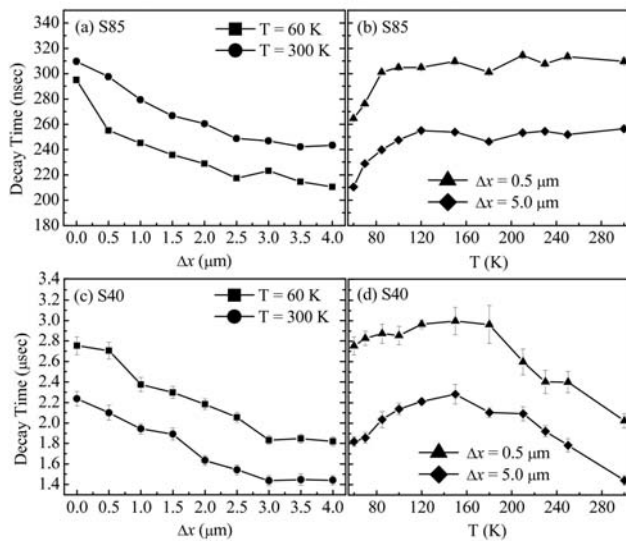
Figure 5 CL decay times of the ground state QD excitonic recombination as a function of distance Δx from a microcrack in (a) and (c) and as a function of temperature in (b) and (d) for both samples S85 and S40.

temperature range is at first glance somewhat perplexing since the reduction of the nonradiative components at lower temperature ought to increase the overall decay time. However, again we consider the ever increasing thermal tensile stress of the epilayer film as the temperature is lowered in the $120 \geq T \geq 60$ K range. The increasing thermal tensile stress of the AlN barriers is expected to reduce the compressive stress of the GaN QDs, thereby resulting again in a reduced electric field responsible for the spatial separation of electrons and holes. Thus, we hypothesize that a field reduction at low temperatures is primarily responsible for an increased oscillator strength and reduced carrier lifetime.

4 Conclusion We have studied the effect of uniaxial stress on the optical polarization properties of vertically stacked GaN/AlN QDs grown on Si(111) substrates. We show that naturally occurring microcracks serve as excellent stressors through which the strain tensor of QDs can be modified for studies of strain-induced changes in the optical properties. The spatial dependence of the polarization anisotropy, R_p, and CL decay time in varying proximity to the microcracks were studied as a function of temperature in order to assess the influence of thermal stress variations. More generally, we expect that the heteroepitaxial growth of a variety of III-V quantum heterolayers on Si substrates will thus create unique opportunities for future studies of self-assembled QDs in close proximity to naturally occurring stressors in the form of microcracks.

References

[1] T. S. Hirayama H. Aoyagi, Y. Narukawa, Y. Kawakami, and S. Fujita, Appl. Phys. Lett. **71**, 1299 (1997).
[2] B. Damilano, N. Grandjean, F. Semond, J. Massies, and M. Leroux, Appl. Phys. Lett. **75**, 962 (1999).
[3] B. Damilano, N. Grandjean, J. Massies, and F. Semond, Appl. Surf. Sci. **164**, 241 (2000).
[4] S. Kalliakos, T. Bretagnon, P. Lefebvre, T. Taliercio, B. Gil, N. Grandjean, B. Damilano, A. Dussaigne, and J. Massies, J. Appl. Phys. **96**, 180 (2004).
[5] A. D. Andreev and E. P. O'Reilly, Phys. Rev. B **62**, 15851 (2000).
[6] L. Liu and J. H. Edgar, Mater. Sci. Eng. R **37**, 61-127 (2002).
[7] A. Dadgar, A. Strittmatter, J. Bläsing, M. Poschenrieder, O. Contreras, P. Veit, T. Riemann, F. Bertram, A. Reiher, A. Krtschil, A. Diez1, T. Hempel, T. Finger, A. Kasic, M. Schubert, D. Bimberg, F. A. Ponce, J. Christen, and A. Krost, Phys. Status Solidi C **0**, 1583 (2003).
[8] D. H. Rich, A. Ksendzov, R. W. Terhune, F. J. Grunthaner, B. A. Wilson, H. Shen, M. Dutta, S. M. Vernon, and T. M. Dixon, Phys. Rev B **43**, 6836 (1991).
[9] G. Sarusi, O. Moshe, S. Khatsevich, D. H. Rich, and B. Damilano, Phys. Rev. B **75**, 075306 (2007).
[10] O. Moshe, D. H. Rich, B. Damilano, and J. Massies, Phys. Rev. B **77**, 155322 (2008).
[11] B. Daudin, F. Widmann, G. Feuillet, Y. Samson, M. Arlery, and J. L. Rouviere, Phys. Rev. B **56**, R7069 (1997).
[12] M. Miyamura, K. Tachibana, and Y. Arakawa, Appl. Phys. Lett. **80**, 3937 (2002).
[13] H. T. Lin, D. H. Rich, A. Konkar, P. Chen, and A. Madhukar, J. Appl. Phys. **81**, 3186 (1997).